REPORT DOCUMENTATION PAGE

Form Approved
OMB No. 0704-0188

1. REPORT DATE *(DD-MM-YYYY)*	2. REPORT DATE	3. DATES COVERED *(From - To)*
07/31/03	Annual Report	07/01/02-06/30/03

4. TITLE AND SUBTITLE
Second Annual Report (AR2)

5a. CONTRACT NUMBER

5b. GRANT NUMBER
N00014-01-1-0634

5c. PROGRAM ELEMENT NUMBER

6. AUTHOR(S)
Juan Carlos Balda, Fred D. Barlow, Panneer Selvam, Aicha Elshabini

5d. PROJECT NUMBER
01PR07524-00

5e. TASK NUMBER

5f. WORK UNIT NUMBER

7. PERFORMING ORGANIZATION NAME(S) AND ADDRESS(ES)
University of Arkansas
Office of Contracts and Grants
Fayetteville, AR 72701

8. PERFORMING ORGANIZATION REPORT NUMBER

9. SPONSORING/MONITORING AGENCY NAME(S) AND ADDRESS(ES)
Mr. Dominic Troiano
Office of Naval Research
Ballston Centre Tower One
800 North Quincy Street, Arlington VA 22217-5660

10. SPONSOR/MONITOR'S ACRONYM(S)
ONR

11. SPONSORING/MONITORING AGENCY REPORT NUMBER

12. DISTRIBUTION AVAILABILITY STATEMENT
Approved for public release, distribution unlimited

13. SUPPLEMENTARY NOTES

14. ABSTRACT
This Second Annual Report summarizes the activities performed on this grant from July 1, 2002, through June 30, 2003. The main technical activities during this time period were the following: (1) Understanding of direct cooling methods for power semiconductors; (2) Themal simulation of spray-cooled power modules; (3) Design of a spray-cool test bed for power modules; (4) Design of experiments for thermal test die; (5) Analysis of selected inverter topologies for high-power motor drives for ship propulsion; and (6) In-depth analysis of a simple method for series connection of IGBTs.

15. SUBJECT TERMS
direct cooling, spray cooling, power modules, inverter topologies, semiconductors

16. SECURITY CLASSIFICATION OF:			17. LIMITATION OF ABSTRACT	18. NUMBER OF PAGES	19a. NAME OF RESPONSIBLE PERSON
a. REPORT	b. ABSTRACT	c. THIS PAGE			Juan Carlos Balda
UU	UU	UU	UU	23	19b. TELEPONE NUMBER *(Include area code)* 479-575-6578

DIRECT COOLING OF PROPULSION DRIVES

FOR HIGH POWER DENSITY AND LOW VOLUME

Award No. N00014-01-1-0634

Period of Performance: July 01, 2002 – June 30, 2003

Second Annual Report (AR2)

Juan Carlos Balda, Fred D. Barlow, Panneer Selvam, Aicha Elshabini

University of Arkansas
Department of Electrical Engineering
3217 Bell Engineering Center
Fayetteville, AR 72701–1201
(501) 575-3005

Prepared for

Office of Naval Research
Ballston Center Tower One
800 North Quincy Street
Arlington, VA 222A-5660

July 2003

INTRODUCTION

This Second Annual Report summarizes the activities performed on this grant from July 1, 2002, through June 30, 2003.

The research team consisted of Drs. J. C. Balda, F. D. Barlow, R. P. Selvam (Department of Civil Engineering) and A. Elshabini, and graduate students Habib Mustain (doctoral candidate), Yanan Wei (doctoral candidate), Kiramkumar Vanam (doctoral candidate), Bhavesh Joshi (MS candidate) and Jeremy Junghans (MS candidate). Mr. Mustain, Mr. Vanam and Mr. Junghans worked on the overall direct cooling system design and packaging philosophy of our spray-cooled power module. Mr. Joshi worked for a semester on some aspects of liquid cooling. Mrs. Wei investigated different inverter topologies and series connection of IGBTs in order to reduce the power losses of high-power motor drive systems, and thus, to reduce the thermal load of the chillers. The selected example is an induction motor drive rated 24 MW and 4.16 kV (line-to-line). In other words, the product of the thermal resistance times the power losses gives the temperature increase in the power semiconductor devices. Mr. Mustain and Mr. Vanam tackled the thermal resistance issue from the cooling and packaging technology side while Mrs. Wei tackled the power loss issue from the system side. This dual approach should yield an optimized solution for high-power motor drive systems used for ship propulsion. Mr. Junghans aided with the experimental test bench.

MAIN TECHNICAL ACTIVITIES FROM JULY 1, 2002, TO JUNE 30, 2003

The main technical activities performed during this time period were the following:

- Understanding of direct cooling methods for power semiconductors;
- Thermal simulation of spray-cooled power modules;
- Design of a spray-cool test bed for power modules;
- Design of experiments for thermal test die;
- Analysis of selected inverter topologies for high-power motor drives for ship propulsion; and
- In-depth analysis of a simple method for series connection of IGBTs (we will report on this method once that experimental results become available).

SPRAY COOLING RESEARCH

The vision of the future Electric Warship requires significant reductions in size and weight of shipboard electronically-controlled electric motors and actuators (i.e., increased power densities). A key problem with power modules today is the very high power densities that result in significant problems with thermal management. Traditionally, high thermal conductivity materials have been used to overcome this problem by reducing the thermal resistance between the heat source(s) and the heat sink or cooling system. However, this methodology has some fundamental limitations due to the thermal conductivity of materials as well as the interfaces that inevitably exist within a module. An alternative approach is the use of a direct cooling method to extract the waste heat (i.e., power losses) from the power semiconductor devices. Many investigations have been conducted to take advantage of phase change heat transfer. These include pool boiling, jet impingement, falling-film cooling and micro heat exchangers [1-8]. Such processes take advantage of the fact that a component will absorb or release a substantial quantity of heat at a fixed temperature during its phase change process. Several approaches have been explored; however, the most effective technique is spray cooling. Spray cooling has the capability of removing higher heat fluxes through phase change, which provides many opportunities for future electronic cooling systems. It offers heat flux values, about ten times higher that that of pool boiling methods and over one hundred times higher than conventional fan and heat sink cooling. Fig. 1 shows the comparison of spray cooling to pool boiling and convection cooling. A key element of this work is to explore the implementation of spray cooling for high-power systems.

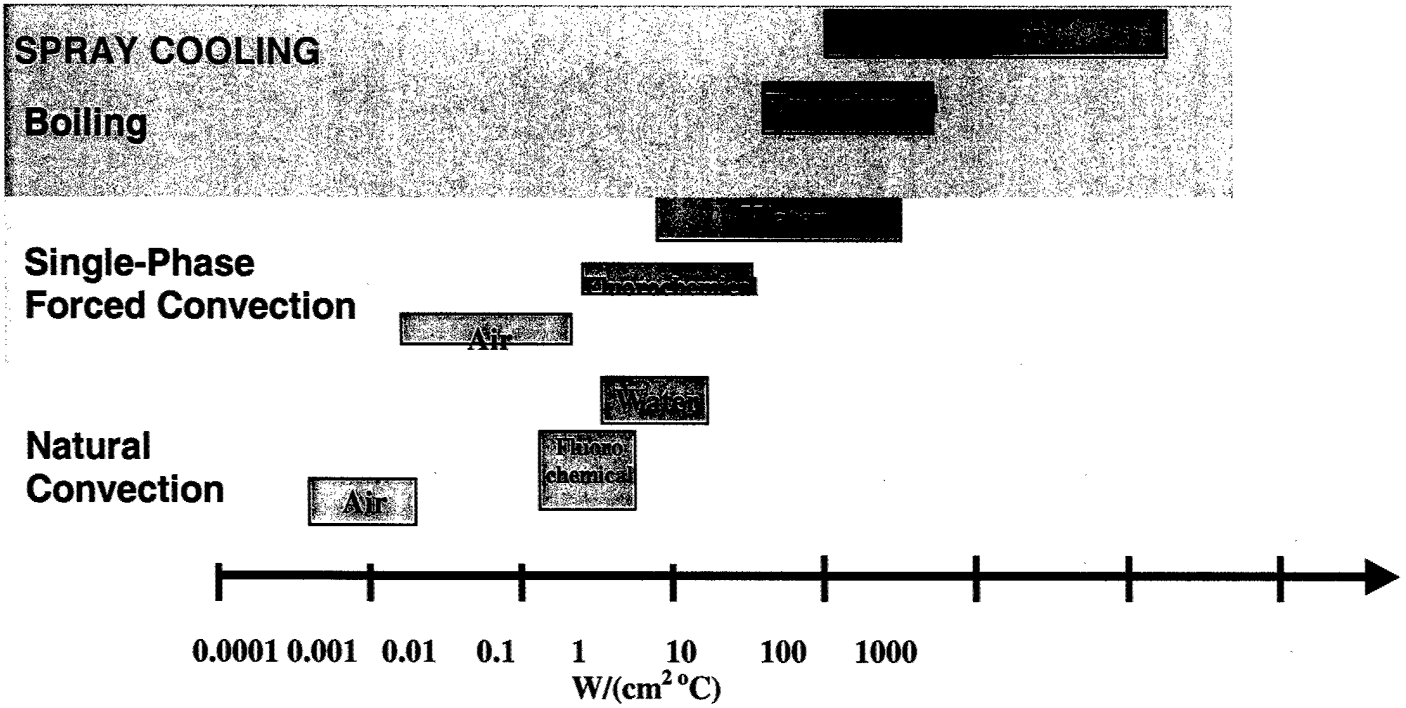

Figure 1 Comparison of the different possible cooling methods and their relative performance.

This task of the project includes the optimization of a spray-cooling system for power electronic modules as well as the development of a packaging methodology for the electronic components within the module.

Spray Cooling Basics

Conventional high-power systems normally employ power modules that are mounted to heat sinks in order to provide adequate thermal management. Depending on the power level, these systems may use forced air convection or liquid cooled cold plates (see Fig. 2). However, a thermal resistance exists between the devices and the cooling media (air or liquid) in all of these cases. Spray cooling directly cools the active components within a system via a dielectric liquid. The most effective direct cooling systems would utilize boiling rather than convection as the dominant cooling method, due to the greater cooling efficiency associated with the boiling process [1]. In the case considered in this section, the liquid is sprayed as a mist on the object to be cooled. On contact the liquid boils removing the heat as a vapor. The systems then utilizes a heat exchanger to condense the vapor back into the liquid state and then recycle it back into the liquid spray stream.

Fig. 2 provides a comparison of a conventional liquid cooled system versus a spray-cooled system. Note the components on the left hand side are common to both types of systems (although they may have different ratings). Both techniques require a pumping system to circulate the cooling liquid and heat exchangers to extract the heat load to the external environment. Both configurations also require an expansion or liquid storage tank. For the spray cooling technique this tank also serves as the housing of the system. The primary difference is in the interface between the module and the cooling system. The liquid-cooled approach utilizes a cold plate where the cooling liquid circulates through and the power module(s) are mounted on. The spray cooling approach utilizes a spray head that directs onto the components to be cooled the flow of liquid.

Two fundamental advantages exist in the spray-cooled approach, the potential lack of thermal resistance between the components to be cooled and the cooling liquid, and the heat of vaporization effect. The lack of thermal resistance arises from the application of the cooling liquid directly to the devices in question rather than to the back of a substrate or heat spreader. Since the liquid boils at this surface the heat of vaporization is removed from the device resulting in a higher cooling efficiency. The key question is how to implement this type of system for naval applications.

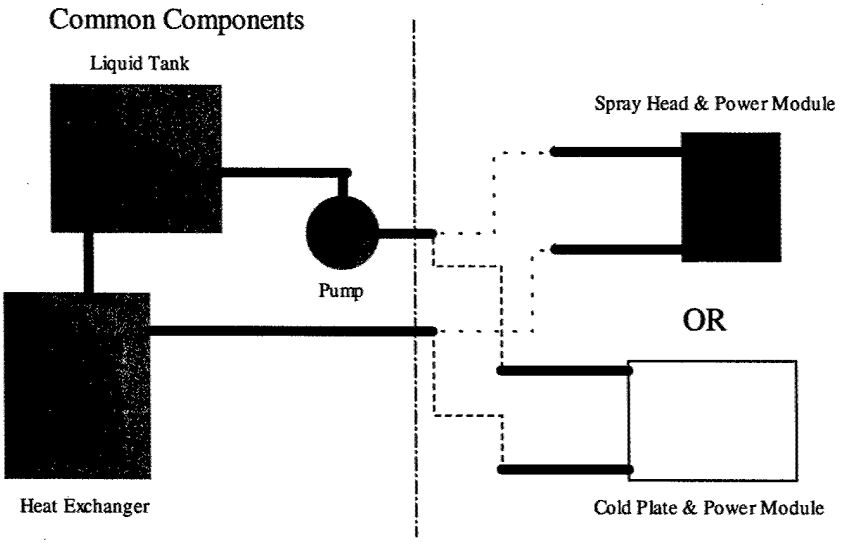

Figure 2 Block diagram of spray cooled and liquid cooled power systems.

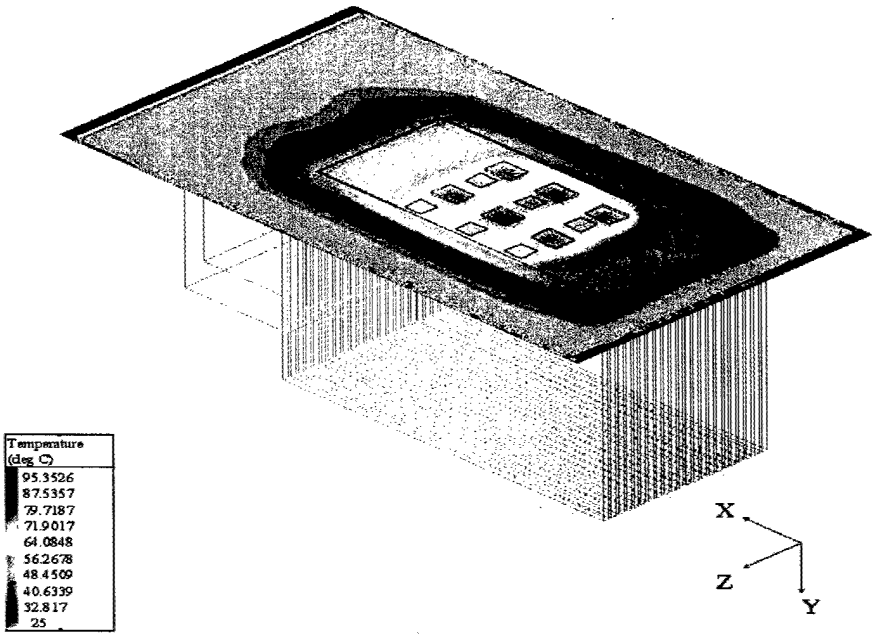

Figure 3 A thermal model of an inverter power module using forced convection.

Thermal Modeling

In order to determine the optimum methodology for spray cooling, the ability to model the thermal performance is vital. As a result, the researchers have developed a preliminary model for a spray-cooled power module commonly used for motor drives. The module consists of six (6) IGBTs and six (6) freewheeling diodes mounted on a Direct Bond Copper (DBC) substrate. This model, illustrated in Fig. 3, has been explored with conventional convective cooling as well as with spray cooling. Fig. 3 illustrates the typical behavior observed for this configuration using a finned heat sink under forced convection conditions. Fig. 4 summarizes the behavior of this module as a function of power loss in the active devices. In comparison, identical modules have been modeled using spray cooling. This work has been done for a range of heat transfer coefficients. From reports in the literature, it is possible to achieve heat transfer coefficients as high as 30,000 [W/m^2 °C] using this technique. Fig. 5 illustrates the performance of a power module (identical to the module in Fig. 3) with 500 W of thermal loss for a range of heat transfer coefficients h. At 500 W, the junction temperature is approximately 95° C. Therefore, the "breakeven" h value, as compared to conventional cooling, is approximately 10,000 [W/m^2 °C]. For an h value greater than ~15,000 [W/m^2 °C], the performance of the spray-cooled system is far superior to the conventional cooling case. In some cases, junction temperatures may be as much as 50% lower for the spray cooling case. Of course, this has direct and positive implications to power semiconductor device and system reliability since the maximum power density is directly related to the device temperature. These modeling results illustrate the potential of spray cooling to solve some of the thermal management problems that currently exist in high-power electronic systems.

Spray Cooling Test Bed Design

In order to verify these results, the researchers have designed and developed a spray cooling test bed to evaluate the feasibility of spray cooling technique for power modules. This test bed consists of a spray-cooling system that has been modified for high-power modules, departing from an existing system at the University of Arkansas that was originally used to cool VME cards for testing high-density computer modules, Fig. 6. This system has been modified to provide high-power input and output terminals and to replace the standard VME card with a metal card designed to provide universal support for virtually any power module of interest, as seen in Fig. 7.

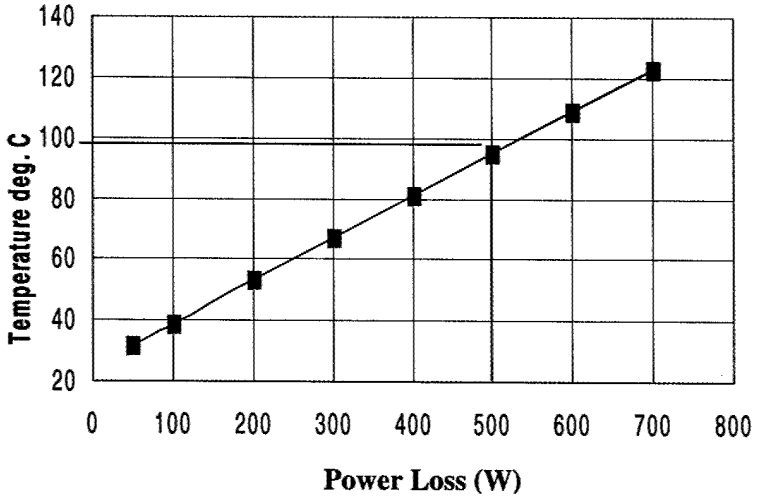

Figure 4 Thermal simulation results for forced convection of a three-phase inverter module (The data is based on junction temperatures as a function of the thermal loss in the module).

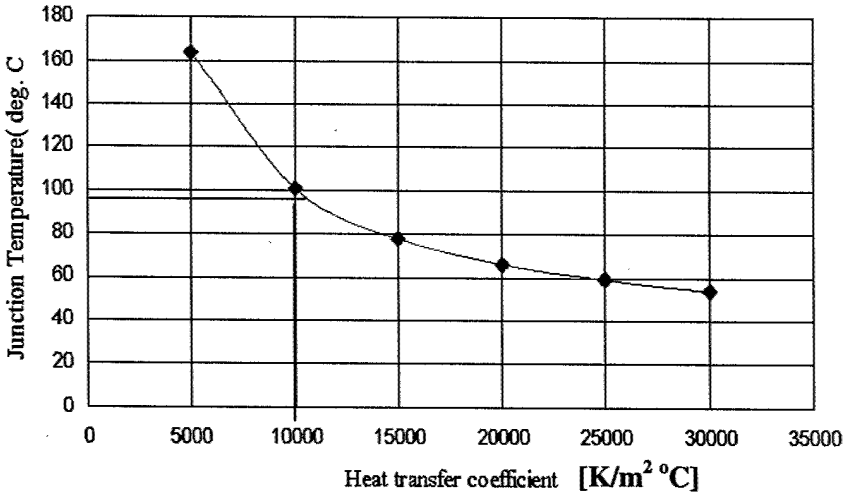

Figure 5 Simulation results for a spray-cooled module operating with 500 W of power loss for a variety of h values.

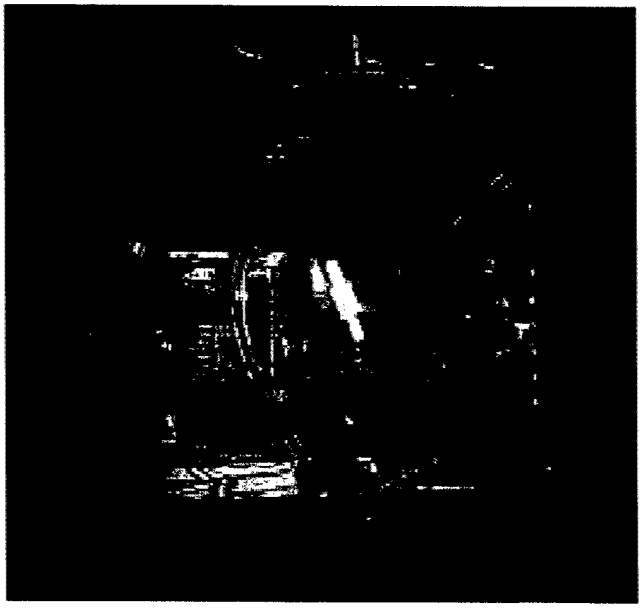

Figure 6 An existing spray cooling system at the University of Arkansas (This system cooled high power digital modules on a VME card).

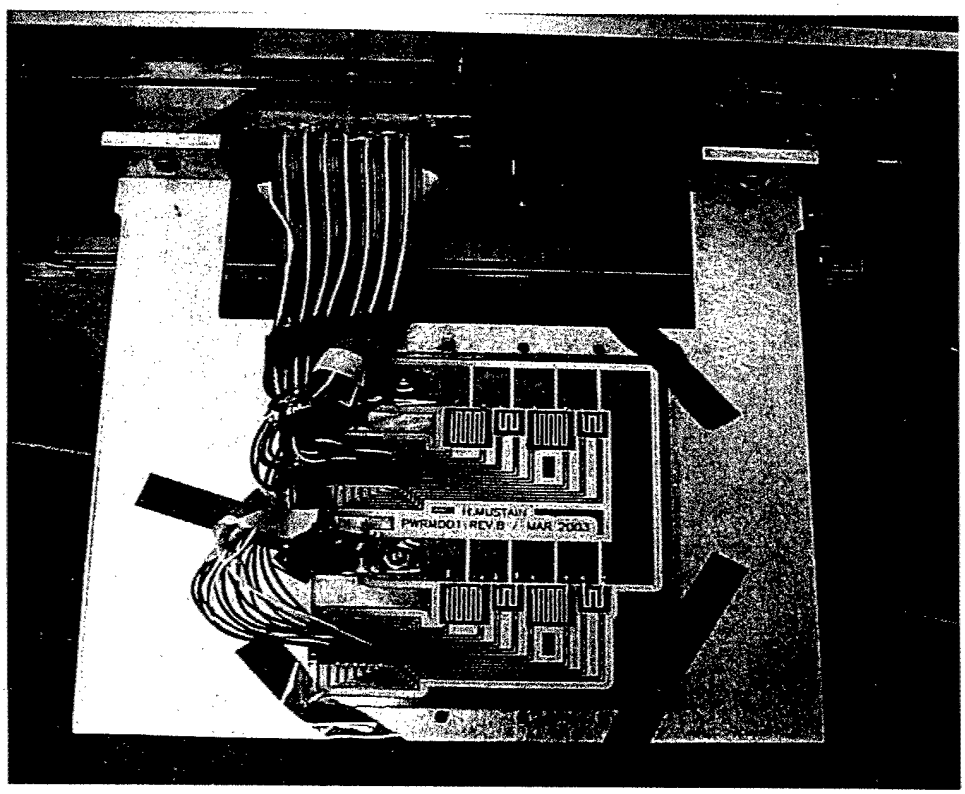

Figure 7 Power module mounted on spray cooling test bed.

Bus bars have been included to provide the high current / high voltage I/O. In addition, a D sub connector is provided for temperature sensor I/O and has been designed to monitor the junction temperatures of the devices within a given power module. A custom spray head has been designed that is suitable for cooling a full (H) bridge power module. The spray head is shown in the Fig. 8. Overall dimensions of the spray head are 5.6 x 2.62 inches.

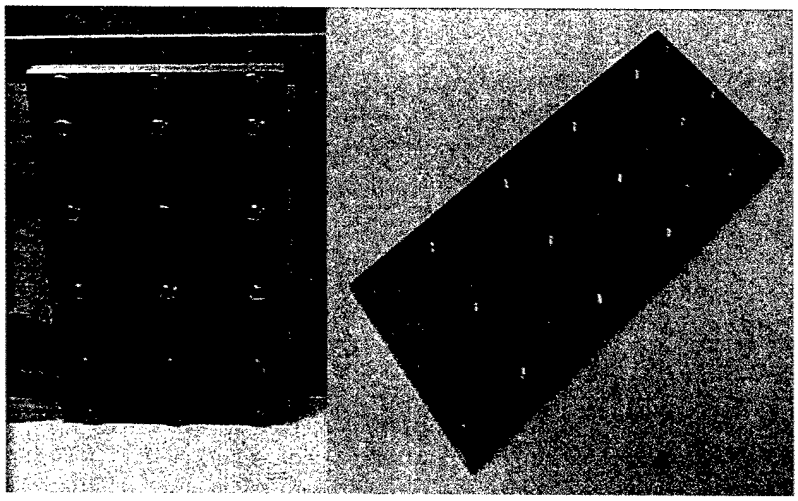

Figure 8 A spray head developed by the researchers for use in power module cooling.

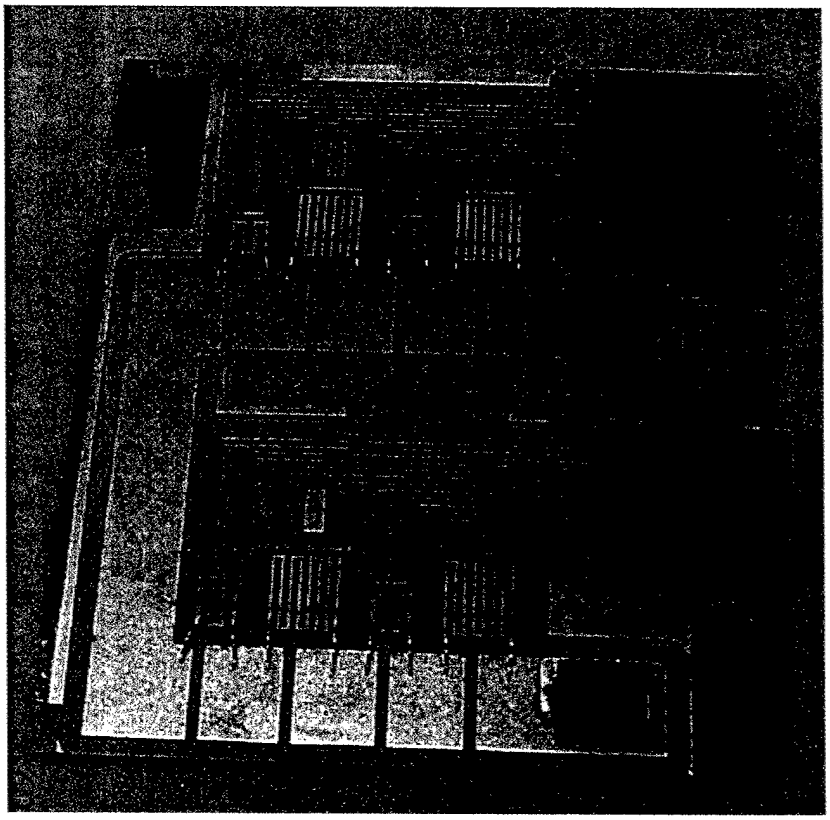

Figure 9 Fabricated power module on a DBC substrate.

The researchers designed a thermal test module as the initial application for this test bed. This module, illustrated in Fig. 7, consists of an IMS substrate and eight (8) thermal test die. Two types of test die were used. One die design simulates an IGBT and is 0.564 x 0.564 inches in size, the second design simulates the thermal properties of a diode and is 0.366 x 0.366 inches in size. Each test chip includes temperature sensors that monitor the top surface temperature (i.e., the junction temperature) of each device. The researchers have also fabricated similar substrates based on Direct Bond Copper (DBC) Alumina and AlN, as shown in Fig. 9. These substrates will enable far higher power densities than the IMS and PCB based designs, and they are currently undergoing evaluation.

Experimental Setup

The experimental setup is pictured in Fig. 10. A dielectric fluid (fluorinert) is directly sprayed from the spray nozzle onto the devices. The liquid droplets impinge on the heated surface and form a thin film. This film is heated and evaporates from the surface. The evaporated fluid condenses on the walls of the spray box and gets collected at the bottom of the spray box. The fluid is then passed through a heat exchanger where the excess heat is removed and the fluid is again pumped back onto device in a continuous cycle. By ramping the power loss in the device and monitoring the junction temperature, the researchers were able to verify their thermal models. The following procedure was followed to run the experiments. The nozzle pressure was set to the desired value and the nozzle was centered and placed at the required height from the power module. At this point, the power to the test die was gradually increased at a slow rate. Thermal stability was ensured before data points were acquired between each step. Finally, when the Critical Heat Flux (CHF) was reached, the test die power was turned off.

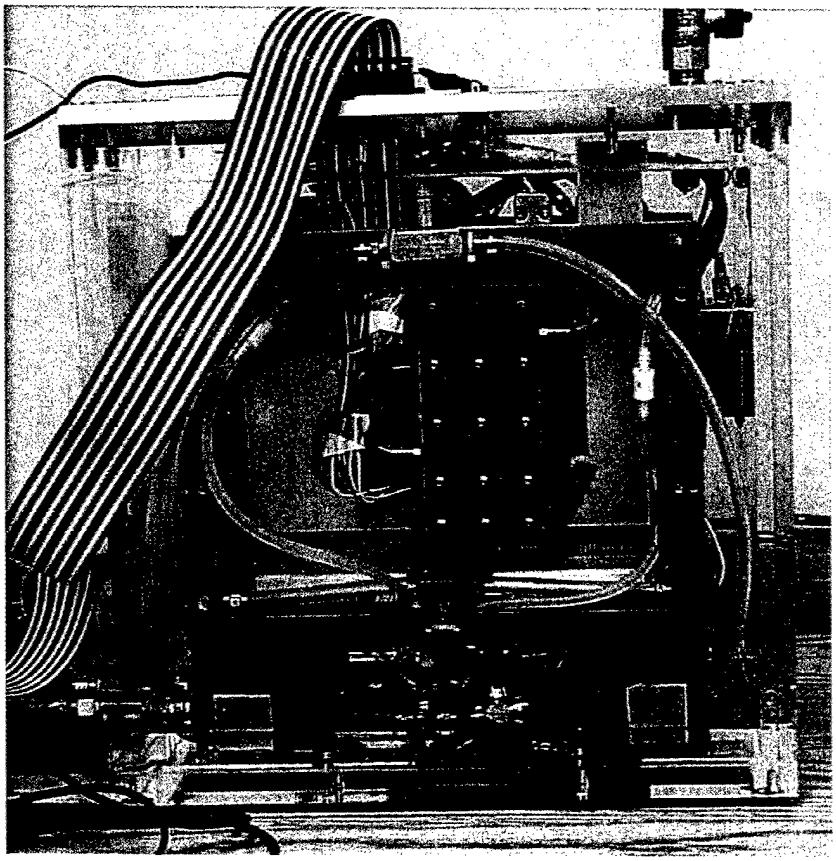

Figure 10 Experimental setup of the spray cooling test bed.

This occurs when the liquid on the surface dries out completely and the temperature rises rapidly. After the power was turned off, the spray was continuously supplied until the heater cooled down to room temperature. This procedure was repeated for different spraying conditions.

Experimental Results

Initial experiments based on a power module built on FR-4 yielded a maximum power dissipation of 181 W. This would correspond to a system power level of 3.62 kW, assuming an efficiency of 95%. Experiments were also conducted on an IMS board using spray nozzles instead of a spray head. The maximum power dissipation yielded 476 W. This corresponds to a system power level 9.5 kW. Both substrates were only a few square inches in size. The spray nozzles used in this work were Spraying Systems Unijet full cone TG series, as well as the nozzles developed by the researchers. These nozzles are pressure spray designs where in fluid is supplied at high pressures through a small orifice. Parameters that affect the cooling phenomenon such as spraying pressure, nozzle to surface distance and orientation of the substrate were also investigated. The results are shown in the Figs. 11-13 and were also compared with research done by I. Mudawar [9]. The initial work illustrates the potential of spray cooling over conventional cooling techniques and with further work much better results can be achieved. The researchers are also planning to use water as the spraying liquid as it has better thermo physical properties which results in higher heat flux values in the order of 1000 W/cm^2 [10]. The effects of the working fluid temperature, the substrate (DBC Alumina and Aluminum nitride), nozzle orifice diameter and spray velocity on the heat transfer mechanism are also to be investigated.

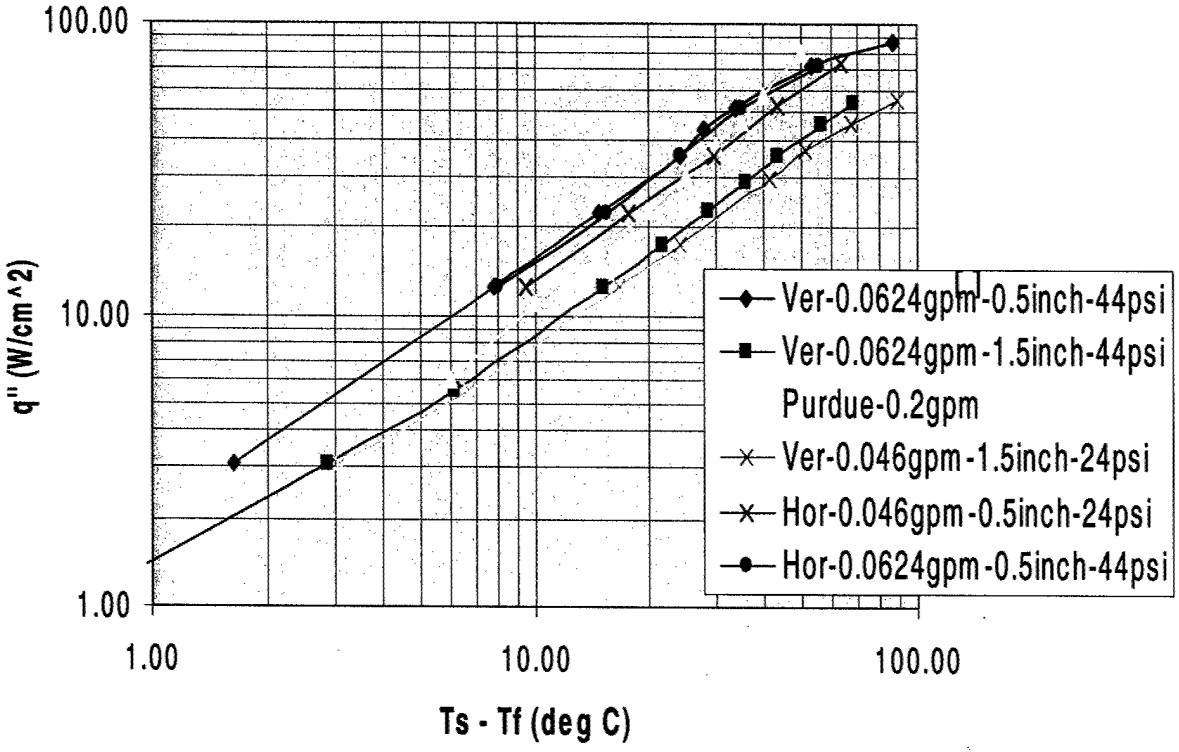

Figure 11 Effect of variation in power module orientation, pressure and distance on heat flux (log scale). The legend indicates the orientation of the module, flow rate, distance from the nozzle to device and pressure.

The variation of heat flux with temperature difference (between the surface of the device and fluid temperature) is depicted in Fig. 11. These plots are for different pressures, nozzle to surface distances and spraying orientation (vertical = "ver" or horizontal="hor" in the legend). The results obtained by the researchers at Purdue are also shown [9]. The figure illustrates that heat flux reached a maximum of 86 W/cm^2 when the nozzle distance was at 0.5 inch and the pressure was 44 psi at a flow rate of 0.624 gpm in the vertical spraying position of the power module. Higher pressures result in greater flow rate as such volumetric flux of the spray was increased and this in turn increased the heat flux. Also the closer the distance of the nozzle to the surface to be cooled the greater the percentage of the fluid that reached the surface. This increase in percentage of the fluid enhances the heat flux. This nozzle to surface effect is depicted in Fig. 12. If a single nozzle is used then the nozzle to surface distance should be as such that the spray area just covers the device that is being cooled. If multiple nozzles are used then the distance at which the fine drops are completely realized from the nozzle will govern the minimum distance. It can also be observed from the figure that the orientation of the power module (vertical or horizontal) has very little effect on heat flux for the same pressure and nozzle to surface distance. This effect may not be true at all power levels since in some cases pooling of coolant, which would reduce the heat transfer rate, may occur for modules in the horizontal position when sprayed from above.

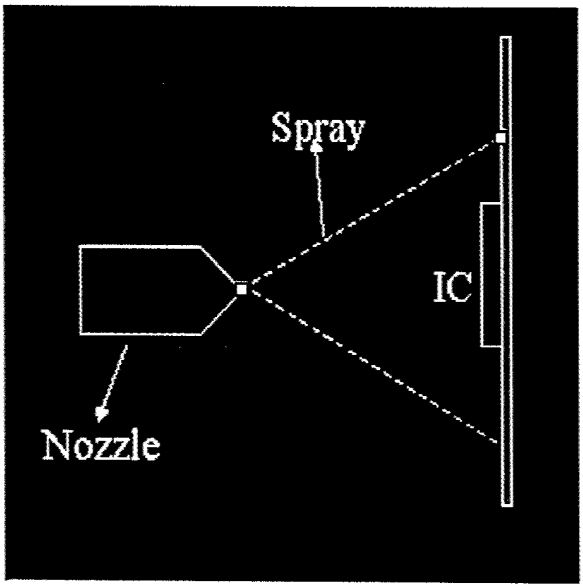

Case I: Relatively lower percentage of working fluid reaching the surface of the device.

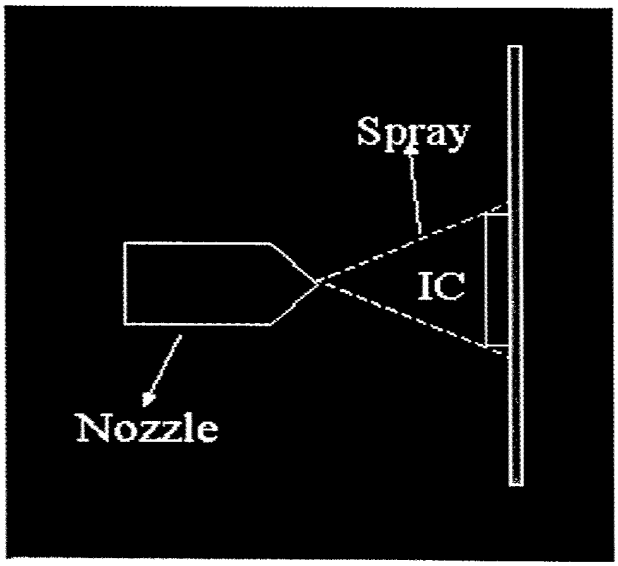

Case II: Higher percentage of working fluid reaching the surface of the device.

Figure 12 Different nozzle to surface distance scenarios.

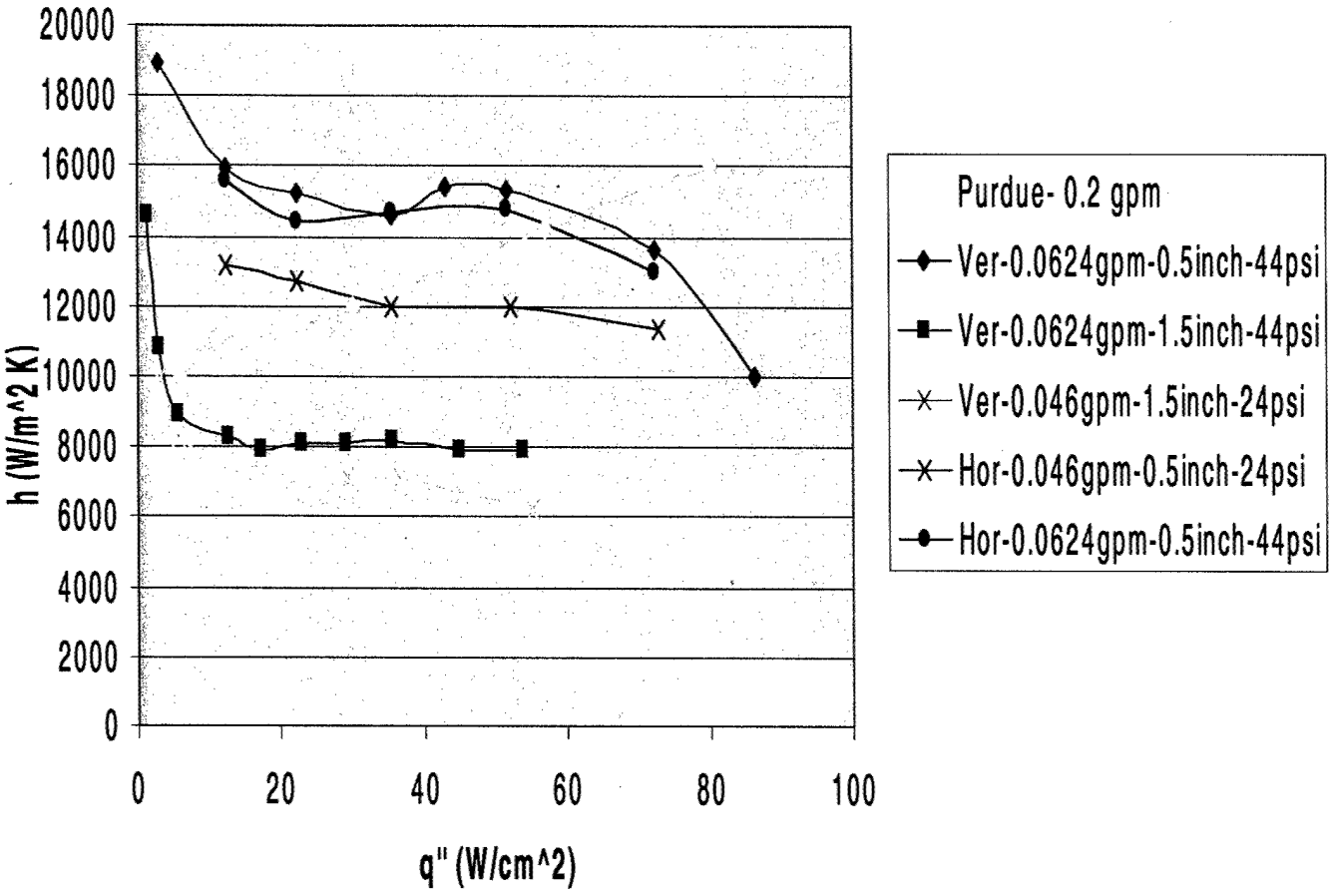

Figure 13 Heat transfer coefficient vs. heat flux.

Fig. 13 demonstrates the variation of heat transfer coefficient with heat flux. The heat transfer value drops with higher heat flux. This might be due the attainment of the critical heat flux for the nozzle that was used in this work.

IMPORTANT CONSIDERATIONS FOR HIGH POWER MOTOR DRIVES SYSTEMS FOR SHIP PROPULSION

Ship propulsion requires motor drives rated in the megawatt level (e.g., 24-MW) usually connected to a medium-voltage network (e.g., 4.16-kV). High power levels increase the current rating of the power semiconductor devices for a given dc-bus voltage. Above certain current levels, devices must be paralleled leading to the issue of equally sharing the load current in order to not exceed the device maximum current. Using higher dc-bus voltages (for example, 6-kV) reduces the current ratings and thus requires paralleling fewer devices. However, series connections of the devices become necessary above certain dc-bus voltage levels in order to not exceed the device ratings recommended by the manufacturers [11-12].

Multi-level inverter topologies [13-16] reduce the maximum voltage applied to the devices but not their current rating for given dc-bus voltage and number of phases. The three-level inverter three-phase motor drive system is the most common topology commercially available [16]. In principle, this three-level inverter, which operates with a split-voltage dc bus, offers two important advantages over the conventional two-level counterpart; namely:

1. The voltage stress on each device is only half of the total dc-bus voltage (under normal operating conditions). Thus, higher dc-bus voltage levels can be obtained by using devices of lower voltage ratings (but higher current ratings).
2. The increased number of stepped voltage levels at the inverter output leads to better voltage waveforms that in turn reduce the Total Harmonic Distortion (THD) and filtering efforts.

In addition to increase the dc-bus voltage level, increasing the number of phases can reduce the number of paralleled devices further. For example, the rated current in a six-phase induction motor is half of the rated current in a three-phase induction motor having the same power and voltage ratings. A six-phase induction motor has two sets of three-phase windings (that are spatially phase shifted by either 30 or 60 electrical degrees), and improves the reliability of the system (since losing one or more inverter phases may not prevent the motor from starting or running). Also, the six-phase system allows selecting more inverter voltage vectors to eliminate common-mode voltage generated by PWM operation. A three-level, three-phase (3L3P) inverter has only seven voltage vectors with zero common-mode voltage [17-20]. A three-level six-phase (3L6P) inverter has 49 zero common-mode voltage vectors. Thus, the 3L6P system has more flexibility.

This report proposes a high-power inverter topology for ship propulsion using a hybrid approach that involves the three-level and six-phase technologies. This approach has the following two important advantages:

1. The three-level system reduces the Total Harmonic Distortion and filtering efforts at the inverter output.
2. The six-phase inverter makes it possible to eliminate completely the common-mode voltage providing larger control flexibility.
3. Fewer devices need to be connected in series/parallel at each switch position making its practical realization simpler than an inverter having two levels and three or six phases. The phase of a two-level inverter has two switch positions, one connecting the positive rail and the other one connecting the negative rail. Similarly, a three-level inverter has four switch positions.

Fig. 14 shows the 3L6P inverter for a propulsion system rated 24-MW and 4.16-kV. The freewheeling diodes were not drawn in order to simplify the diagram. The system specifications are summarized in Table 1. The inverter peak output current includes the startup current of the electric motor and the reverse recovery current of freewheeling diodes in parallel with the IGBTs. Based on the available values, the reverse recovery current is often equal to the load current following through each phase of the inverter. Each switch position may consist of several devices connected in series and/or parallel depending on the device rated current and voltage (see Fig. 15).

Nowadays, Insulated Gate Bipolar Transistors (IGBT) seem more suitable to series connection than other devices because of their capability of switching at relatively high frequencies and high voltage ratings, as well as simple gate control [21]. A judicious choice of the ratings of the devices allows reducing the total inverter losses [22].

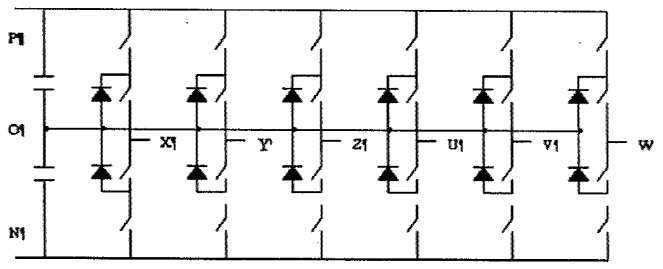

Figure 14 Schematic diagram of a 3L6P inverter.

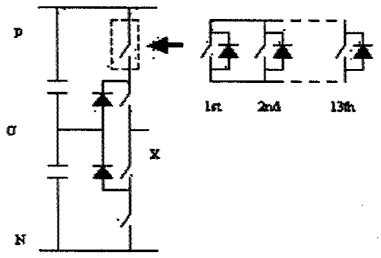

Figure 15 One phase of a 3L6P inverter using 3.3-kV 1200-A IGBTs.

Device Comparison

Power Losses

Table 2 compares 2.5-kV 1200-A, 3.3-kV 1200-A, and 6.5-kV 600-A IGBTs for the 3L6P inverter selected for the 24-MW 4.16-kV drive system. An analysis shows that the device ratings are very important in order to reduce the complexity of each switch position when connecting IGBTs in series and/or parallel and the total inverter losses.

The shorting of an IGBT in a switch position must not cause a voltage greater than the IGBT maximum breakdown voltage to be applied to the healthy IGBT. This condition determines the number of IGBTs connected in series. For example, there are two 3.3-kV 1200-A IGBTs connected in series in each switch position since the manufacturer recommends an operating dc-bus voltage of 1.65 kV. When taking into consideration the peak output current, each switch position needs in parallel 13 of the two-IGBT strings. So, each switch position has 26 IGBTs (that in turn may consists of several bare dies connected in parallel). Figure 15 shows the schematic diagram of one phase of the 3L6P inverter when using 3.3-kV IGBTs. Under the same considerations, the inverter requires in parallel 13 strings having now three IGBTs in series for each switching position when considering the 2.5-kV IGBTs with the recommended voltage of 1.25 kV. There are now 39 IGBTs that make the connection complexity higher. Using devices with higher voltage ratings requires fewer devices and may even eliminate the need for series connection in each switching position for a given dc-bus voltage. In the case of the 6.5-kV IGBT, Table 2 shows that each switch position requires 25 IGBTs connected in parallel eliminating the cumbersome requirement of voltage sharing when connected in series.

Another point to consider is the IGBT losses since each IGBT has different switching and conduction losses. Table 2 compares loss values and maximum switching frequencies in the 3L6P inverter for the three IGBTs under the following working parameters:

1. Maximum junction temperature: $T_J = 125^0 C$ (as specified by the manufacturer)
2. Ambient temperature: $T_A = 40°C$
3. Thermal resistance between the sink and the ambient: $R_{th\_SA} = 0.02^0 C/W$ (liquid cooling)

For the same switching frequency of 0.4 kHz (determined by the maximum junction temperature of the 6.5-kV IGBT), the inverter system with the 3.3-kV IGBTs produces the smallest inverter total losses, 842 kW (reductions of approximately 15% and 70%, respectively, when compared to the other two IGBTs); requires only one additional device with respect to the 6.5- kV IGBT per switch position; and the switching frequency can be increased to 1.4 kHz.

Table 1 Basic specifications of a 3L6P inverter.

Parameters	Value/Type
Nominal DC Input Voltage	$V_{dc} = 6kV$
Output Power	$P_{out} = 24MW$
Power Factor	$PF = 0.86$
Electrical Motor Efficiency	$\eta = 90\%$
Motor Startup Current	$I_{st} = 200\% I_{load}$
Rated Load Current (RMS)	$I_{rated} = 2.15kA$
Peak Load Current	$I_{out\_peak} = 15kA$

I_{load} is the load current of each phase of the inverter

Table 2 Operating values for three different IGBTs in a 3L6P inverter.

IGBT	2.5-kV, 1200-A	3.3-kV, 1200-A	6.5-kV, 600-A
Series/Parallel IGBT	3/13	2/13	1/25
Switching Losses (kW)	223	223	778
Conduction Losses (kW)	743	619	657
Thermal Resistance Junction-Sink (K/W)	0.018	0.018	0.017
Maximum Switching Frequency (kHz)	2.3	1.4	0.4

The switching frequency is 0.4 kHz for the losses calculations, the minimum value of the three maximum switching frequencies.

Hence, using 3.3-kV 1200-A IGBT seems to make more sense in the considered motor drive system when taking into account the connection complexity in each switch position and the total power losses (cooling capacity) of the inverter. The disadvantage is the series connection of two IGBTs

Thermal Load Analysis

The losses generated in the inverter have a great impact on the cooling system technology (e.g., liquid cooling, heat pipes, phase change). According to the thermal/electrical analogies, the *maximum* thermal resistance, R_{th}, of each switch position in order to not exceed the device maximum junction temperature for given power losses (that depend on the switching frequency) can be calculated as follows:

$$R_{th,\max} = \frac{T_j - T_A}{P_{loss}} \tag{1}$$

The corresponding heat flux and *required* "h" heat transfer coefficient for each switch position are as follows:

$$heatflux = \frac{P_{loss}}{A} \tag{2}$$

$$h = \frac{1}{R_{th}\, A} \tag{3}$$

where, A is the IGBT silicon area for each switch position.

The device that requires a smaller heat transfer coefficient "h" allows increasing the power density for given power losses when using a certain cooling technology, and thus, optimizing the system design. For the 24-MW, 4.16-kV system, Table 3 lists the thermal characteristics of the three different IGBTs for the switching frequency of 0.4 kHz. An analysis indicates that the 3L6P inverter using 3.3-kV 1200-A IGBTs requires the smallest heat transfer coefficient "h", 0.9 W/cm^{2}K, which provides a larger freedom to increase the power density of the system and achieve a better system optimization as compared to the other two IGBTs. It is again shown that the appropriate choice of the devices plays an important role in the design of the motor drive system, and the 3.3-kV, 1200-A IGBT would be a better choice for this system. The maximum thermal resistance is the maximum value in order to not exceed the junction temperature of 125°C

Different cooling schemes have different range of heat transfer coefficients. Practical system considerations, like switching frequency that impacts the inverter total losses, have an important effect on selecting a suitable cooling system. Table 4 displays the relevant data for switching frequencies between 500 Hz and 10 kHz using 3.3-kV 1200-A IGBTs assuming a current density of 30 A/cm^2. The researchers realize that switching frequencies greater than 2 kHz are basically not possible for today's motor drives. The aim of the table is to identify the cooling system improvements to allow increasing the switching frequency. All other parameters were given above. The values in Table 4 indicate that the switching frequency is limited to approximately 2 kHz when using a liquid-cooling technology, a mature technology that has approximately $h < 0.9\ W/cm^2K$. In order to improve the motor current waveforms, the switching frequency must be increased, e.g. 5 kHz.

Table 3 Thermal load analysis for different IGBTs at each switch position.

IGBT	Current Density (A/cm^2)	Silicon Area (cm^2)	Power Losses (kW)	Heat Flux (W/cm^2)	Maximum Thermal Resistance (K/W)	Required "h" Coefficient (W/cm^{2}K)
2.5-kV, 1200-A	35	1251	41	33	0.08	0.4
3.3-kV, 1200-A	30	972	35	36	0.06	0.4
6.5-kV, 600-A	27	541	60	111	0.04	1.3

Table 4 Cooling system requirements as function of the switching frequency

Switching Frequency (kHz)	Power Losses (kW)	Heat Flux (W/cm^2)	Maximum Thermal Resistance (K/W)	Required "h" Coefficient (W/cm^2K)
0.5	37	38	0.059	0.4
0.75	43	44	0.051	0.5
1	49	50	0.045	0.6
2	72	74	0.031	0.9
3	95	97	0.023	1.2
4	118	121	0.019	1.4
5	142	146	0.015	1.7
6	165	170	0.013	2.0
7	188	193	0.012	2.3
8	212	218	0.010	2.6
9	235	241	0.009	2.9
10	258	265	0.008	3.2

Correspondently, the heat transfer coefficient "h" of the cooling system must be increased, for example, to *1.7 W/cm^2K* for 5 kHz. However, it is impossible to realize these heat transfer coefficients using a liquid-cooling technology, so, it is necessary to find another efficient cooling system, which has higher "h" values, like phase-change cooling.

Topology Comparison

Comparison With Series H-Bridge Cascade Inverters

The series connected H-bridge multi-level cascade inverter topology is a very attractive approach for high-power motor drive systems [23-24]. Furthermore, the introduction of the Integrated Gate Commutated Thyristors (IGCT), which has high current and voltage ratings, like 5SHY 30L610 (6-kV, 3000-A) IGCT, make it possible to design the series H-bridge multi-level inverter by using IGCTs [25]. In the 24-MW 4.16-kV, 6P system, the multi-level cascade inverter consists of two series connected H-bridge inverter with five parallel-connected IGCTs (6-kV, 3000-A) in each switch position, which realize a cascade inverter with five voltage levels (5L) at each phase output; namely, ±3 kV, ±1.5 kV, 0. Figure 16 shows one phase of the 5L inverter. The primary advantage of the H-bridge cascade inverter is that the problem associated with capacitor voltage balancing (typical of multi-level inverters) is eliminated because of the independent dc voltage source structure. Also, according to the characteristics of the different devices, a high power drive system can be obtained by a hybrid inverter approach [23], simultaneously using IGBT and IGCT in the cascade inverter. But, there are inherent disadvantages as follows:

1. Multiple independent dc voltage sources are required in the system, which make the system expensive [24].
2. The hybrid inverter topology needs to generate two different switching frequencies, one for the IGBT, and the other for the IGCT, so, the complexity of control system is higher [23].
3. The switching frequency of the drive system is limited, because the switching losses of the IGCTs are higher [24].
4. The complexity of the gate drive for a 3000-A IGCT is higher [25].

Comparison With Flying Capacitor Converters (FCC)

A flying capacitor converter uses floating capacitors to share the dc voltage [24]. Fig. 17 shows a 5L flying capacitor converter. Similarly to the cascade configuration, this topology eliminates the unbalanced capacitor voltage problem because of the independent dc voltage sources across the floating capacitors.

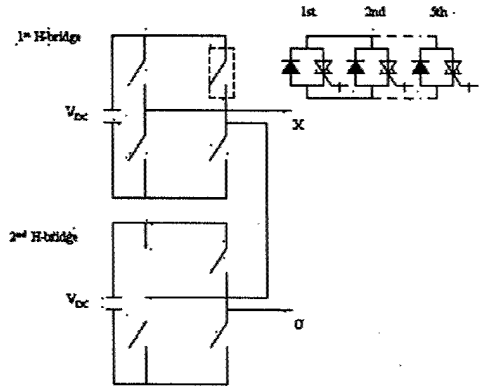

Figure 16 Schematic of one phase of the series H-bridge cascade inverter.

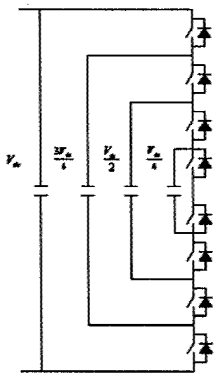

Figure 17 One phase of the 5L FCC.

However, the different voltage levels, as shown in Fig. 17, not only make the system more expensive, but also require a complicated voltage regulation strategy. Especially, in the 24-MW 4.16-kV system, the maximum voltage across one of the floating capacitors reaches to 6 kV, such a high voltage rating has to require several capacitors connected in series, which cause the number of capacitors to increase dramatically.

CONCLUSIONS

The main goal of this work was to demonstrate the potential of spray cooling and identify the spray parameters and their effects on the heat transfer process. More exhaustive work needs to be done to optimize the spray cooling process. The mechanism for CHF for different spraying conditions is yet to be determined.

From the experiments, the following conclusions can be drawn

(1) Higher pressures ensure high heat flux

(2) The heat flux value was improved with the increase in percentage of fluid reaching and covering the device by adjusting the distance of the nozzle.

(3) The initial work revealed that the spray cooling technique is the best option for cooling power semiconductor devices. A heat flux of 86 W/cm^2 was achieved using fluorinert as the working fluid. Using other fluids with better thermophysical properties and optimizing the spraying parameters can boost this value tremendously.

This report also presented important considerations for high-power motor drive systems:

(4) Choosing the appropriate IGBTs was useful to reduce the complexity of the device connection in a switch position and the total inverter losses, in turn, leading to smaller heat transfer coefficients "h". The device comparisons indicated the 3.3-kV, 1200-A IGBT would be preferred for the 24-MW 4.16-kV system.

(5) The thermal load analysis indicated that the cooling system with a higher heat transfer coefficient needed to be developed in order to improve the motor current waveforms.

(6) Different topology comparison showed that the cascade multi-level inverter and flying capacitor converter were limited to the system voltages below the one considered in this application because of the complicated control strategy and switching frequency limitation.

KEY MILESTONES

Using the original Gantt chart, the researchers have accomplished the following:

Task 1.0 – Technical Specifications of the Power Semiconductor Modules

Sub-task 1.1 – Assimilate SOTA for HV IGBT technology
The results of this sub-task were used in the research work to obtain Table 2 above that compared different HV IGBTs for motor drives intended for ship propulsion.

Sub-task 1.2 – Define all electrical specifications
The electrical specifications of the motor drive system have been defined in Table 1 above. However, the research work involving the electrical specification of a "power module" still continues since it closely related to the spray-cooling characterization. In other words, a power module could be thought of a switch position in an inverter (see definition in this report). At high power levels, the switch position consists of several IGBT bare dies connected in parallel (and perhaps in series). For example, a switch position for the 24-MW, 4.16-kV motor drive system could have around 550 bare dies (connected in series and in parallel). It is difficult to include these many bare dies in a single power module, even using standard packaging technology. Then, it is important to establish if one nozzle is needed for each bare die or a nozzle can spray several bare dies. This is important in order to establish the basic electrical structure of a power module. Thus, the research work continues in this sub-task.

Sub-task 1.3 – Define all mechanical specifications
Same comments as those in sub-task 1.2.

Sub-task 1.4 – Define all thermal specifications
This research work is ongoing due to the feedback that naturally takes place as the researcher move forward in this project. The heat flux depends on the IGBT used (see Table 3 above) and also the switching frequency (see Table 4 above).

Task 2.0 – Design of Spray-Vapor Cooling for IGBT-based Power Modules

Sub-task 2.1 – Direct cooling development
This research work is ongoing. So far, the researchers have developed a test bench to experimentally characterize spray cooling. This report presented the results of the initial experimental work.

Sub-task 2.2 – Electronic packaging
This research work has just begun since the power packaging methodology depends on the spray cooling approach. The researchers will be reporting in the future on two power packaging methods being investigated.

Task 3.0 – Integrated Gate Driver Design

Sub-task 3.1 – Construct a lumped-charged model of the HV IGBT
The research work in this area is completed. The researchers performed PSpice simulations of series connected IGBTs in order to develop high-power inverter systems using IGBTs of lower rated voltages but more efficient than those IGBTs of higher rated voltages (see Table 2 above).

Sub-task 3.2 – Electrical characterization of the HV IGBT
This research work is completed. The researchers characterized the IGBT using PSpice.

Sub-task 3.3 – Design HV IGBT gate driver circuits
The researchers have developed a gate driver that is fiber-optic isolated as used in High-Voltage (HV) IGBTs.

Sub-task 3.4 – Perform an electro-thermal simulation of the HV IGBT gate drive design
This research work is ongoing.

Sub-task 3.5 – Iterative refinement on the HV IGBT driver electrical design
This research work, closely related to sub-task 3.3, is completed and the researchers anticipate reporting by December 2003.

Sub-task 3.6 – HV IGBT driver layout
Same comment as that in sub-task 3.5.

Task 4.0 – Prototyping and Testing

Sub-task 4.1 – HV IGBT gate driver fabrication
The driver printed circuit boards are being fabricated at the writing of this report.

Sub-task 4.2 – HV IGBT gate driver testing
This research work will take place during the Fall 2003.

FUTURE EFFORTS

The researchers have developed the following revised plan based on their results, which is summarized in the Gantt chart on the next page:

- Experiments indicate that increased pressure and flow rate result in a larger maximum heat flux value. These results have previously been limited by the experimental setup. The researchers will eliminate this constraint by replacing the existing pump with one capable of greater pressure and flow rates. Additional changes include the addition of a liquid chiller and upgrade of the heat exchanger to eliminate the fluctuation in the fluid temperature. The current instrumentation will be upgraded to allow the researchers to vary the pressure and flow rate over a wider range while reducing the error in experimental measurements.
- The theory behind the spray cooling phenomenon will be explored and a mathematical model will be generated for the system of interest.
- The researchers will continue work on the electronic packaging of the spray cooled power module. The researchers have identified several methods of packaging the power module. Modeling will be used to for thermal and stress analysis of each method. Prototypes of each packaging method will be built and tested thoroughly.
- A paper design of the spray cooled 24-MW six-phase inverter will be produced, incorporating the chosen method of electronic packaging.
- A scaled down in power version of the above 24-MW inverter will be fabricated and tested for a selected packaging schemes and overall cooling efficiency.
- Experimental work of the series-connected IGBTs will be carried out to gain experience on the IGBT responses.

ID	Task Name	Start	Finish
1	**Evaluate High Power DBC Spray Cooled Test Module**	**Wed 7/2/03**	**Fri 8/29/03**
2	**DBC AlN Module Fabrication**	**Wed 7/2/03**	**Thu 7/3/03**
3	Assembly	Wed 7/2/03	Wed 7/2/03
4	Acoustic Microscopy	Wed 7/2/03	Wed 7/2/03
5	Final Wirebond Attachment	Thu 7/3/03	Thu 7/3/03
6	Experimental Evaluation	Mon 7/7/03	Fri 8/1/03
7	Improved Pump Selection	Wed 7/2/03	Mon 7/7/03
8	Heat Exchanger Upgrade	Wed 7/2/03	Mon 7/7/03
9	Instrumentation Upgrades	Wed 7/2/03	Mon 7/7/03
10	Apply Mathematical Theory of Spray Cooling	Wed 7/2/03	Fri 8/29/03
11	**Electronic packaging**	**Wed 7/2/03**	**Wed 12/31/03**
12	Thermal and Stress Analysis Proposed Package Structures	Wed 7/2/03	Wed 7/16/03
13	Build/ Develop Proposed Package Structures I, II, III	Fri 8/1/03	Fri 11/14/03
14	Testing	Mon 11/17/03	Wed 12/31/03
15	**Paper Design**	**Tue 7/1/03**	**Mon 1/26/04**
16	Design Spray Cooled 24 MW Six Phase Inverter	Tue 7/1/03	Tue 7/1/03
17	Design Scaled down version	Thu 1/1/04	Mon 1/26/04
18	**Fabricate Scaled Down Inverter**	**Tue 1/27/04**	**Wed 3/31/04**
19	Build Scaled Inverter Design	Tue 1/27/04	Fri 2/27/04
20	Testing and Evaluation	Mon 3/1/04	Wed 3/31/04
21	**Three-Level Six-Phase IM Drive Modeling**	**Thu 5/1/03**	**Thu 7/31/03**
22	Selection of the converter topology for drive	Thu 5/1/03	Mon 6/30/03
23	Six phase IM Modeling	Tue 7/1/03	Thu 7/31/03
24	**Three-Level Six-Phase IM Drive Control**	**Mon 6/2/03**	**Fri 10/31/03**
25	Development of the PWM technique	Mon 6/2/03	Fri 8/15/03
26	Development of the control scheme	Mon 8/18/03	Fri 10/31/03
27	**IM Drive Prototype- Discrete Components**	**Mon 11/3/03**	**Thu 4/1/04**
28	Prototype Fabrication	Mon 11/3/03	Wed 12/31/03
29	Prototype Testing	Thu 1/1/04	Thu 4/1/04

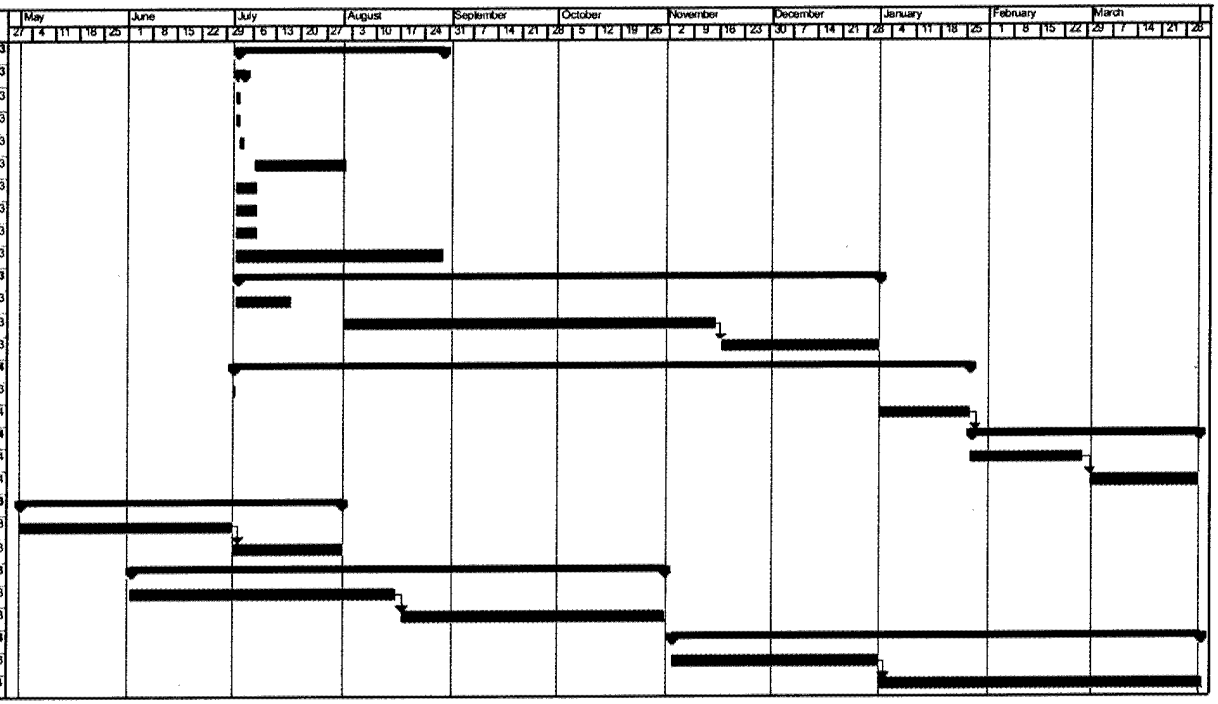

REFERENCES

[1] M. C. Shaw, J. R.Waldrop, B. Chandrasekaran, B. Kagalwala, X. Jing, "Enhanced Thermal Management by Direct Water Spray of High Voltage, High Power Devices in Three-Phase, 18-hp AC Motor Drive Demonstration", *2002 IEEE Inter Society Conference on Thermal Phenomena*, pp. 1007-1113.

[2] E. Bigzadeh, F. Mignano, "Experimental Determination of Heat Transfer Coefficient with Spray Cooling", *Proceedings of the ASME Heat Transfer and Fluids Engineering Divisions*, Vol. 233, pp. 73-88, 1995.

[3] L, Ortiz, J. E. Gonzalez, "Experiments on steady-state high heat fluxes using spray cooling", *Experimental Heat Transfer*, Vol. 12, No. 3, pp. 215-233, 1999.

[4] E. I. Caroll, "Power Electronics for very high power applications", *ABB Review*, Vol. 2, pp. 4-11, 1999.

[5] A. P. Bhansali, W. Z. Black, "Local Instantaneous Heat Transfer Coefficients for Jet Impingement on a Phase Change Surface", *Journal of Heat Transfer*, Vol. 118, No.2, 1996.

[6] M. S. Sehmbey, L. C. Chow, M. R. Pais, "High Heat Flux Spray Cooling- A review", *Journal of ASME, Heat transfer in High Heat Flux Systems*, HTD-Vol. 301, 1994.

[7] A. Marcos, L. C. Chow, Jian-Hua Du, Shuye Lei, D. P. Rini, J. J. Linauer, "Spray Cooling at Low system pressure", *18th Annual IEEE Symposium on Semiconductor Thermal Measurement and Management*, March 12-14 2002, pp.169-175.

[8] Chulin Xia, "Spray/Jet cooling for heat flux high to 1 kW/cm^2", *Semiconductor Thermal Measurement and Management*, 2002. 18th Annual IEEE Symposium, 12-14 March 2002, pp.159-163.

[9] I. Mudawar, "Assessment of High-Heat-Flux Thermal Management Schemes", *IEEE Transactions on Components and Packaging Technologies*, Vol. 24, No. 2, pp. 122-141, June 2001.

[10] K. Kiger, Jungho, H. Bohumil, E. Silk, "Project: Spray and Droplet Cooling", *University of Maryland*, College Park, http://www.enme.umd.edu/~kimjh

[11] S. Kaufmann, F. Zwick, "10 kV IGBT Press Pack Modules with series connected chips", *14th International Symposium on Power Semiconductor Devices and ICs*, June 4-7, 2002, pp. 89-91.

[12] C. H. Yang, Y. C. Liang, "Investigation on parallel operations of IGBTs", *IEEE International Conference on Industrial Electronics, Control, and Instrumentation*, vol. 2, August, 1996, pp. 1005-1010.

[13] J. Rodriguez, J. S. Lai, F. Z. Peng, " Multi-level inverters: a survey of topologies control, and applications," *IEEE Transactions on Industrial Electronics*, vol. 49, No. 4, 2002, pp. 724-735.

[14] A. Nagel, S. Bernet, P. K. Steimer, O. Apeldoorn, "A 24 MVA inverter using IGCT series connection for medium voltage applications," *Conference Record of the 2001 IEEE Industry Applications Annual Meeting*, vol. 2, 2001, pp. 867-870.

[15] P. K. Steimer, M. D. Manjrekar, "Practical medium voltage converter topologies for high power applications," *Conference Record of the 2001 IEEE Industry Applications Annual Meeting*, vol. 3, 2001, pp. 1723-1730.

[16] R.Sommer, A. Mertens, M. Griggs, H. J. Conraths, M. Bruckmann, T. Greif, "New medium voltage drive systems using three-level neutral point clamped inverter with high voltage IGBT," *Conference Record of the 1999 IEEE Industry Applications Annual Meeting*, vol. 3, 1999, pp. 1513-1519.

[17] Y. Zhao, T. A. Lipo, "Space vector PWM control of dual three-phase induction machine using vector space decomposition," *IEEE* Transactions *on Industry Applications*. vol. 31, No. 5, 1995, pp. 1100-1109

[18] R. H. Nelson, P. C. Krause, "Induction machine analysis for arbitrary displacement between multiple winding sets," *IEEE Transactions on Power Application and System*, vol. PAS-93, 1974, pp. 841-848.

[19] M. J. Costello, " Shaft voltage and rotating machinery." *IEEE Transactions on Industry Applications,* vol. 29, No. 2, 1993, pp. 419-426.

[20] H. Zhang, A. V. Jouanne, S. Dai, A. K. Wallace, F. Wang, "Multi-level inverter modulation schemes to eliminate common-mode voltages." *IEEE Transactions on Industry Applications,* vol. 36, No. 6, November/December, 2000, pp. 1645-1653.

[21] J. W. Baek, D. W. Yoo, H.G. Kim, "High Voltage Switch Using Series-Connected IGBTs with Simple Auxiliary Circuit", *IEEE Transactions on Industry Applications,* Vol. 37, No. 6, Dec. 2001, pp. 1832-1839.

[22] H. V. Blavi, L. M. Salamero, J. Maixe, E. V. Idiarte, "Optimizing losses in Multi-level inverters," *IEEE 28th Annual Conference of the Industrial Electronics Society,* vol. 1, 2002, pp. 846-851.

[23] M. D. Manjrekar, P. Steimer, T. A. Lipo, "Hybrid Multi-level power conversion system: a competitive solution for high power application", *IEEE Transactions on Industry Applications*, vol. 36, No. 3, 2000, pp. 834-841.

[24] B. S. Suh, G. Sinha, M. D. Manjrekar, T. A. Lipo, "Multi-level power conversion-an overview of topologies and modulation strategies", *Proceedings of the OPTM'98 Conference,* 1998, pp. AD-11-AD-24.

[25] S. Bernet, "Recent developments of high power converters for industry and traction applications", *IEEE Transactions on Power Electronics,* vol. 15, No. 6, 2000, pp. 1102-1117.